

# PHYSICAL REVIEW E

STATISTICAL PHYSICS, PLASMAS, FLUIDS,  
AND RELATED INTERDISCIPLINARY TOPICS

THIRD SERIES, VOLUME 52, NUMBER 3 PART B

SEPTEMBER 1995

## ARTICLES

### Observation of $KL \rightarrow LL$ x-ray satellites of aluminum in femtosecond laser-produced plasmas

J.-C. Gauthier, J.-P. Geindre, P. Audebert, and A. Rousse\*

*Laboratoire pour l'Utilisation des Lasers Intenses, Ecole Polytechnique, 91128 Palaiseau, France*

A. Dos Santos, G. Grillon, and A. Antonetti

*Laboratoire d'Optique Appliquée, Batterie de l'Yvette, Ecole Nationale des Sciences et Techniques Avancées,  
91120 Palaiseau, France*

R. C. Mancini

*Department of Physics, University of Nevada, Reno, Nevada 89557-0058*

(Received 22 February 1995)

The aluminum  $KL$  satellite emission spectrum excited by suprathermal electrons originating from the nonlinear interaction of a high intensity subpicosecond laser pulse with a solid target is obtained. The measured integrated intensity of the  $KL \rightarrow LL$  satellites relative to the  $K\alpha$  line is found to be 30% higher than in previous experiments performed with continuous, monoenergetic electron excitation. A double-vacancy creation by the shake-off process and a two step inner-shell ionization mechanism are investigated to interpret the data. An upper estimate of the preheating electron temperature is deduced from the analysis.

PACS number(s): 52.50.Jm, 52.40.Nk, 32.30.Rj, 32.80.Hd

#### INTRODUCTION

The development of bright and ultrafast x-ray sources from picosecond and subpicosecond laser-produced plasmas has shown very rapid progress in recent years [1–3]. Thermal x-ray emission from the weakly expanding, high density ( $> 10^{22} \text{ cm}^{-3}$ ) hot plasma (100–1000 eV) produced by focusing an intense ( $> 10^{16} \text{ W/cm}^2$ ), short pulse (0.1–1 ps) laser has been measured (for a review see Ref. [3]) and characterized [4–6] in many laboratories. For low- $Z$  elements ( $Z \leq 20$ ),  $K$ -shell radiation from Li-like, He-like, and (for the higher intensities) H-like resonance and satellite lines is predominantly emitted [7–10]. It has been recognized recently that a significant fraction of the laser energy can be absorbed by various nonlinear mechanisms [11,12] to give rise to a distribution of suprathermal electrons. These highly energetic electrons eject inner-shell electrons from the target atoms, which produce fluorescence line radiation [7,13,14] as the inner-shell vacancies are filled from outer shells. High energy

continuum x-ray emission resulting from bremsstrahlung [15] has also been reported. X-ray conversion efficiency in this nonthermal plasma emission component has been measured to be comparable to and even higher than the thermal component [16]. Up to now only  $K\alpha$  emission spectra from neutral and weakly charged ions has been observed [13] in aluminum. Recently, an application of short pulse laser-produced kilovolt radiation to x-ray fluorescence studies has been demonstrated [17].

In this paper, we present an observation of  $KL \rightarrow LL$  satellite emission corresponding to transitions from initial states having one hole in the  $K$  shell and one hole in the  $L$  shell. We note that our measured  $KL$  satellite to  $K\alpha$  line ratio is only 30% higher than the one obtained earlier by continuous x-ray tube electron excitation [18], despite the fact that our electron excitation is of a highly transient nature. A two-step inner-shell ionization process is investigated to account for the difference.

#### EXPERIMENTAL RESULTS

A colliding-pulse mode-locked dye laser delivering 80 fs duration, 2 mJ energy, and 10 Hz repetition rate laser pulses was focused at intensities ranging from  $10^{16}$ – $10^{17} \text{ W/cm}^2$  onto thin aluminum layers deposited on a silicate substrate. Most of our experimental x-ray recording sys-

\*Present address: Laser Science Group, Institute of Physical and Chemical Research (RIKEN), Hirosawa 2-1, Wako-shi, Saitama 351-01, Japan.

tem and plasma characterization procedures have been described [9,10,13,16] previously. In particular, we have found that the energy distribution of the suprathermal electrons was Maxwellian with an effective temperature of 4–10 keV for laser intensities in the  $10^{16}$ – $5 \times 10^{16}$  W/cm<sup>2</sup> range [13,19]. Being produced by highly non-linear effects, suprathermal electrons are thought to last no longer than the pulse duration. We note that our x-ray spectrograph has been absolutely calibrated against a conventional electron-beam x-ray source [20]. We have shown [10] that Be-like to He-like resonance and dielectronic satellite spectra recorded in the 1500–1600 eV region with a very thin (20 nm) aluminum layer and a thick (> 1000 nm) aluminum target exhibit very different line profiles. In the first case, the spectrum is characteristic of the emission of a hot, expanding plasma with narrow shifted  $K\alpha$  spectral features. In the second case, the  $K$ -shell lines are Stark broadened, indicating that the emission occurs in quasisolid density plasma regions.

In the present experiments, thin targets were made of a 20 nm aluminum layer deposited on a silicate substrate. Thick targets used a 20 nm titanium layer on top of a 400 nm aluminum layer. The purpose of the titanium layer was to exclude from the aluminum spectra the contribution of the hot, expanding plasma [10]. Looking to the 1475–1525 eV range, near the Al  $I K\alpha$  line, we have found a striking difference between the spectra recorded with thin and thick aluminum layers. Figure 1 shows a comparison of the spectra recorded with the two kinds of targets over the whole  $K$ -shell emission energy range. For the thinner target, the shifted  $K\alpha$  transitions of O-like ( $\approx 1500$  eV) to Li-like ( $\approx 1580$  eV) ions are clearly visible, together with the intense Al-like  $K\alpha$  line. We note that the  $K\alpha$  feature consists in fact of many transitions from Al-like to F-like ions, the line contribution of which are blended, as evidenced by the double peak structure seen in Fig. 1 [21]. For the thicker target, O-like to B-like emission features are missing, but we can see the largely Stark broadened Be-like (near 1560 eV) and Li-like (near 1580 eV) features. The peak slightly below 1500 eV cannot be attributed to O-like  $K \rightarrow L$  transitions. Indeed, this can be interpreted as a  $KL \rightarrow LL$  transition involving  $(1s2s)^{-1}$  and  $(1s2p)^{-1}$  vacancies

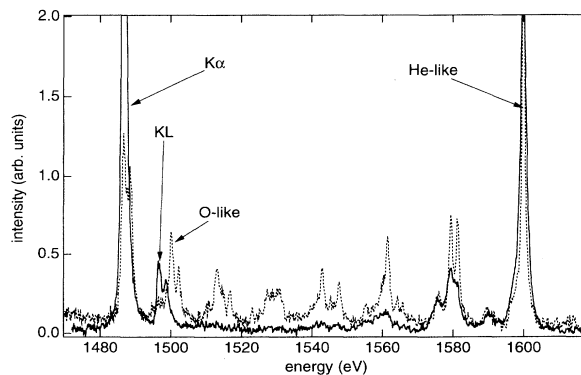


FIG. 1. Comparison of two spectra obtained with 20 nm (dashed line) and 400 nm (solid line) of aluminum at  $3 \times 10^{16}$  W/cm<sup>2</sup>. We note the energy difference of the  $KL$  satellite and of the O-like shifted  $K\alpha$  line around 1500 eV.

[18]. Very weak  $KLL \rightarrow LLL$  transitions around 1510 eV are also barely visible.

We have studied the variations of the  $KL \rightarrow LL$  transition intensity for different experimental conditions, in which we have varied the laser pulse duration and target layer arrangement. Figure 2 shows the results. For a 40 nm titanium overcoat, curves (a) and (b) show the evolution of the  $K\alpha$  satellite when the laser pulse duration was changed from 95 to 230 fs. For a  $\approx 80$  fs laser pulse duration, curves (a) and (c) show the effect of changing the titanium overcoat thickness from 40 to 20 nm. No significant changes in the relative intensity of the  $\alpha_3(1s^{-1}2p^{-1})^3P \rightarrow (2p^{-1}2p^{-1})^3P$  and  $\alpha_4(1s^{-1}2p^{-1})^1P \rightarrow (2p^{-1}2p^{-1})^1D$  peaks (we use the line labeling of Agarwal [22]) was noticed. This indicates that the satellite excitation efficiency is weakly dependent on changes of laser irradiation or target conditions, even if the suprathermal electron energy distribution is changed from its titanium-free determination [13]. This can be expected from earlier measurements of secondary electron emission following x-ray photoionization of the  $K$  shell in

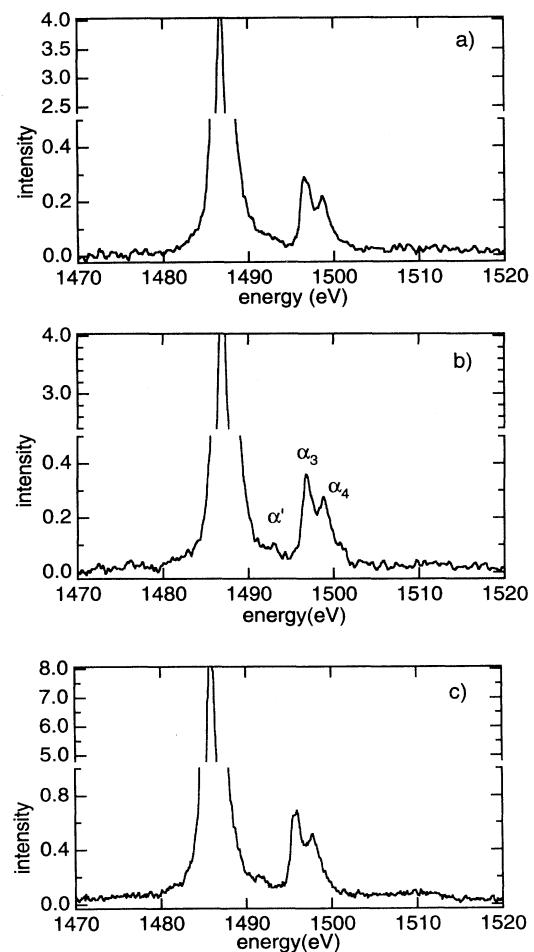


FIG. 2. Detailed spectra of the  $KL \rightarrow LL$  satellites for different experimental conditions. Emission intensity is given in arb. units, (a) 40 nm Ti/400 nm Al, 95 fs laser; (b) 40 nm Ti/400 nm Al, 230 fs; (c) 20 nm Ti/400 nm Al, 90 fs. Laser intensity:  $3 \times 10^{16}$  W/cm<sup>2</sup>.

TABLE I. Measured transient ( $FS$ ) and continuous ( $DC$ )  $KL$  satellite intensity (in percentage of the  $K\alpha$  line) compared to theory.

$FS^a$	$FS^b$	$FS^c$	$DC^d$	$DC^e$	Theory
$12.9 \pm 1.8$	$13.1 \pm 2.4$	$13.95 \pm 3.04$	$10.2 \pm 0.05$	$11.7 \pm 0.03$	8.9

<sup>a</sup>40 nm Ti, 230 fs.

<sup>b</sup>40 nm Ti, 95 fs.

<sup>c</sup>20 nm Ti, 80 fs.

<sup>d</sup>Krause and Ferreira [24].

<sup>e</sup>Mikkola *et al.* [18].

neon [23]. The shake-off probability of ejecting simultaneously a  $K$  and an  $L$  electron was found to be independent of the secondary electron energy (and thus of the ionizing particle energy) for energies larger than twice the threshold, a condition that is fulfilled in our experiments. We note that we also barely observe the  $\alpha'(1s^{-1}2p^{-1})^1P \rightarrow (2p^{-1}2p^{-1})^1S$  peak with an energy difference (5.5 eV) to the  $K\alpha$  line, in very good agreement with a previous experimental determination [18].

We have measured the intensity ratio of the  $KL \rightarrow LL$  satellite to the  $K \rightarrow L$  parent line. Results are given in Table I together with earlier measurements using continuous x-ray tube electron excitation. We observe that the present values obtained with  $\approx 100$  fs duration electron excitation are higher than those obtained in dc conditions. The relative intensity ratio of the  $\alpha_4$  to  $\alpha_3$  peaks is of the order of  $0.75 \pm 0.03$ , a value that is intermediate between the pure aluminum (0.43) and the aluminum oxide (0.91) values quoted in Ref. [24]. The theoretical estimate of the  $KL \rightarrow LL$  to  $K \rightarrow L$  line intensity ratio calculated by Åberg [25] is also given in Table I. Theory predicts about 80% of the observed  $KL$  intensity under dc excitation conditions and 65% of the observed  $KL$  intensity in our highly transient conditions.

### ANALYSIS OF THE RESULTS

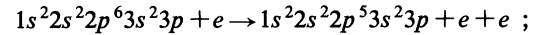
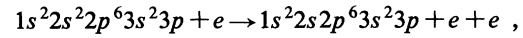
The  $K$  x-ray satellite spectra have been analyzed previously within the framework of the sudden perturbation approximation [23,25]. The intensities of the groups of multiplet transitions are calculated relative to the  $K\alpha$  line from simple formulas [26]

$$\frac{I(1s2s)}{I(1s)} = W(2s) \frac{\bar{w}(1s2s)}{\bar{w}(1s)}, \quad (1)$$

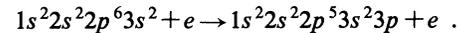
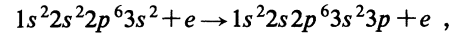
$$\frac{I(1s2p)}{I(1s)} = W(2p) \frac{\bar{w}(1s2p)}{\bar{w}(1s)} \left\{ 1 + \frac{W(2s)\Gamma(2s)}{W(2p)\Gamma(1s2s)} \right\}, \quad (2)$$

where the  $W(nl)$  are the shake-off probability ratios of double to single hole states [25],  $\bar{w}(nl, \dots)$  are the average fluorescence yields, and  $\Gamma(nl, \dots)$  are the widths of levels with holes in the  $(nl, \dots)$  subshells [27]. Application of Eq. (2) to the case of aluminum gives the result in the last column of Table I. However, physical conditions for  $K\alpha$  satellite excitation by a monoenergetic, continuous, photon or electron beam and by a distribution of suprathreshold electrons from a subpicosecond laser-produced plasma are obviously very different. Indeed, the large electron flux originating from nonlinear effects in the expanding plasma deposits its energy deeply

behind the titanium layer and heats the aluminum layer to temperatures that might be sufficient to excite the atoms collisionally. Figure 3 shows a schematic Grotrian diagram of the configurations involved for  $K \rightarrow L$  and  $KL \rightarrow LL$  transitions. A two-step excitation process of the  $(1s2s)^{-1}$  and  $(1s2p)^{-1}$  upper configurations of the  $K\alpha$  satellite becomes feasible if the electron temperature of the bulk target is sufficiently high. First, we can have excitation of the  $(2s)^{-1}$  and  $(2p)^{-1}$  “hollow” configurations from the Al I ground levels by collisional inner-shell ionization:



and by collisional excitation from the Al II ground levels:



Second, we have the removal of one additional  $K$ -shell electron from the  $(2s)^{-1}$  and  $(2p)^{-1}$  “hollow” configurations by the suprathreshold electrons that populate the upper levels of the  $KL$  satellite transitions. The threshold energy for the first process is about 75 eV. For this process to be significant, the ionization rates from the ground Al I to the  $L$ -shell vacancy configurations have to be high enough to ensure collisional equilibrium among the levels in the short time scale of the laser pulse duration. An estimate of the aluminum temperature can be obtained from the absolute measurement of the  $K\alpha$  line and Monte Carlo calculations of electron energy

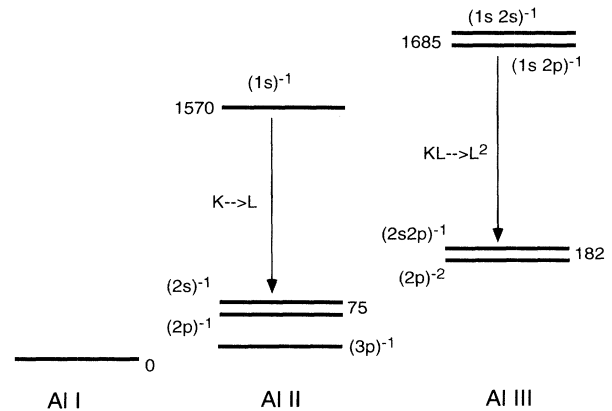


FIG. 3. Simplified Grotrian diagram of the vacancy levels in Al I to Al III. Energies relative to the ground Al I configuration are given.

deposition [20]. Assuming a  $\approx 8$  keV effective temperature for the suprathermal electrons, we get a temperature for the aluminum layer of  $15 \pm 8$  eV.

A theoretical spectrum was constructed by using transition energies, oscillator strengths, Auger rates, and inner-shell collisional ionization and excitation cross sections calculated with the HULLAC atomic physics package of computer programs [28–30]. Fluorescence yields  $\bar{\omega}(1s)$  and  $\bar{\omega}(1s2l)$  were found to be in good agreement with published values [27,31]. Inner-shell ionization rates describing the processes

$$1s^2 2s^2 2p^6 3s^2 3p + e \rightarrow 1s 2s^2 2p^6 3s^2 3p + e + e ,$$

$$1s^2 2s 2p^6 3s^2 3p + e \rightarrow 1s 2s 2p^6 3s^2 3p + e + e ,$$

$$1s^2 2s^2 2p^5 3s^2 3p + e \rightarrow 1s 2s^2 2p^5 3s^2 3p + e + e$$

were found to be equal within 10% when statistically averaged over the lower configuration levels. Accordingly, the population limiting factors of the  $(1s2s)^{-1}$  and  $(1s2p)^{-1}$  “hollow” configurations are the ionization rates to remove one  $n = 2$  subshell electron. These rates, calculated by using the distorted wave Coulomb-Born approximation corrected for electronic correlations [32], are given in Table II as a function of electron temperature.

The intensity of the *KL* group of satellites is calculated relative to the *K $\alpha$*  line from the formula

$$\frac{I(1s2l)}{I(1s)} = \frac{N(1s^2 2l^{-1})}{N(1s^2)} \frac{R(1s^2 2l^{-1} \rightarrow 1s 2l^{-1})}{N(1s^2 \rightarrow 1s)} \times \frac{\bar{\omega}(1s 2l^{-1})}{\bar{\omega}(1s)} , \quad (3)$$

where  $N(1s^2 2l^{-1})$  and  $N(1s^2)$  are the populations of the *L*-shell vacancy configurations and the AlI ground configuration, respectively. The  $R(i \rightarrow k)$  symbols are the corresponding *K*-shell ionization rates. A time-dependent collisional-radiative model was built to calculate the relative populations  $N(1s^2 2l^{-1})$  of the  $(2s)^{-1}$  and  $N(1s^2)$  of the  $(2p)^{-1}$  to the AlI ground levels. It incorporates inner-shell ionization, excitation-deexcitation collisions among  $(2s)^{-1}$  and  $(2p)^{-1}$  levels, and radiative decay. The electron temperature was varied between 10 and 30 eV and the electron density kept constant at  $1.8 \times 10^{23} \text{ cm}^{-3}$  ( $Z \approx 3$ ). Figure 4 gives a comparison between the experimental results of Fig. 2 and the synthetic spectrum obtained at  $T_e = 20$  eV. The theoretical spectrum has been normalized to the height of the experimental *K $\alpha$*  peak. The theory excludes the sudden double-vacancy  $(1s2l)^{-1}$  creation process described earlier. Theoretical energies have been shifted by  $-0.8$  eV so that the theoretical *K $\alpha$*  line exactly matched the experiment. As remarked previously [26], the position of the  $\alpha'$  satellite is low by 1 eV, whereas adding the interacting

TABLE II. Ionization rates ( $\text{cm}^3/\text{s}$ ) as a function of electron temperature. The notation  $2s^- 3p^-(1)$  means one hole in the *2s* shell;  $(-, j = \frac{1}{2})$ ,  $(+, j = \frac{3}{2})$ , and (1) means  $J = 1$ . Numbers in square brackets denote power of 10.

$T_e$ (eV)	10	20	30	40	50
$3p^-(\frac{1}{2})-2s^- 3p^-(0)$	0.162[−14]	0.486[−12]	0.621[−11]	0.232[−10]	0.581[−10]
$3p^-(\frac{1}{2})-2s^- 3p^-(1)$	0.332[−14]	0.100[−11]	0.129[−10]	0.485[−10]	0.121[−09]
$3p^-(\frac{1}{2})-2s^- 3p^+(1)$	0.145[−14]	0.439[−12]	0.564[−11]	0.211[−10]	0.528[−10]
$3p^-(\frac{1}{2})-2p^- 3p^-(0)$	0.330[−13]	0.677[−11]	0.492[−10]	0.149[−09]	0.282[−09]
$3p^-(\frac{1}{2})-2p^- 3p^+(0)$	0.201[−13]	0.412[−11]	0.300[−10]	0.911[−10]	0.171[−09]
$3p^-(\frac{1}{2})-2p^- 3p^-(1)$	0.111[−12]	0.228[−10]	0.166[−09]	0.505[−09]	0.952[−09]
$3p^-(\frac{1}{2})-2p^- 3p^-(1)$	0.120[−12]	0.247[−10]	0.179[−09]	0.545[−09]	0.532[−09]
$3p^-(\frac{1}{2})-2p^- 3p^+(1)$	0.263[−13]	0.541[−11]	0.393[−10]	0.119[−09]	0.225[−09]
$3p^-(\frac{1}{2})-2p^+ 3p^-(2)$	0.231[−12]	0.475[−10]	0.345[−09]	0.104[−08]	0.197[−08]
$3p^-(\frac{1}{2})-2p^+ 3p^+(2)$	0.302[−16]	0.620[−14]	0.450[−13]	0.136[−12]	0.258[−12]
$3p^-(\frac{1}{2})-2p^+ 3p^+(2)$	0.373[−13]	0.765[−11]	0.556[−10]	0.168[−09]	0.318[−09]
$3p^+(\frac{3}{2})-2s^- 3p^-(1)$	0.115[−15]	0.152[−12]	0.246[−11]	0.964[−11]	0.249[−10]
$3p^+(\frac{3}{2})-2s^- 3p^+(1)$	0.264[−15]	0.350[−12]	0.565[−11]	0.221[−10]	0.572[−10]
$3p^+(\frac{3}{2})-2s^- 3p^+(2)$	0.395[−14]	0.120[−11]	0.154[−10]	0.580[−10]	0.145[−09]
$3p^+(\frac{3}{2})-2p^- 3p^-(0)$	0.925[−14]	0.190[−11]	0.138[−10]	0.421[−10]	0.797[−10]
$3p^+(\frac{3}{2})-2p^- 3p^+(0)$	0.151[−13]	0.311[−11]	0.227[−10]	0.691[−10]	0.130[−09]
$3p^+(\frac{3}{2})-2p^- 3p^-(1)$	0.248[−13]	0.510[−11]	0.370[−10]	0.112[−09]	0.212[−09]
$3p^+(\frac{3}{2})-2p^- 3p^-(1)$	0.201[−13]	0.413[−11]	0.300[−10]	0.911[−10]	0.171[−09]
$3p^+(\frac{3}{2})-2p^- 3p^+(1)$	0.497[−13]	0.102[−10]	0.741[−10]	0.225[−09]	0.424[−09]
$3p^+(\frac{3}{2})-2p^- 3p^+(1)$	0.668[−13]	0.378[−11]	0.274[−10]	0.835[−10]	0.157[−09]
$3p^+(\frac{3}{2})-2p^+ 3p^+(2)$	0.133[−12]	0.274[−10]	0.199[−09]	0.605[−09]	0.114[−08]
$3p^+(\frac{3}{2})-2p^+ 3p^+(2)$	0.114[−12]	0.234[−10]	0.170[−09]	0.518[−09]	0.978[−09]
$3p^+(\frac{3}{2})-2p^+ 3p^+(3)$	0.188[−12]	0.387[−10]	0.281[−09]	0.854[−09]	0.161[−08]

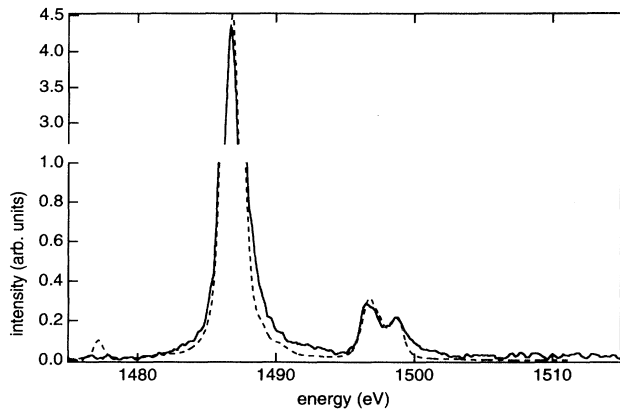


FIG. 4. Comparison of the experimental results of Fig. 2(b) (solid line) with the synthetic spectrum obtained at 20 eV electron temperature (dashed line).

$(2s)^{-2}$  configuration overshoots the experimental value by 1.2 eV. Linewidths were approximated by a Voigt profile, with a Lorentzian width given by the  $\Gamma$  values. Convolution with the 0.5 eV full width at half maximum Gaussian experimental resolution profile was included. We verified that equilibrium populations were obtained in less than 100 fs, the duration of the laser pulse.

Table I shows that the sudden double-vacancy creation process should amount to about 65% of the  $KL \rightarrow LL$  to  $K \rightarrow L$  satellite intensity. This means that the double-step inner-shell ionization process, calculated at 20 eV, overestimates by the same amount the line ratio. We have performed the same calculations with a reduced temperature of 15 eV, and we have added in our model the sudden double-vacancy creation process as calculated by Åberg [25]. The agreement between theory and experiment is similar to the one shown in Fig. 4. However, our time-dependent calculations show that, for an electron temperature of 15 eV, equilibrium populations of the  $(2s)^{-1}$  and  $(2p)^{-1}$  configurations are reached in a time longer than the laser pulse duration. Accordingly, the possibility that target heating effects do not account fully for the removal of the discrepancy between theory and experiment cannot be ruled out. In addition, we have checked that  $K\alpha$  radiation from titanium at 4.5 keV [17] was too small to participate in the  $KL$  satellite excitation by comparing the  $KL$  to  $K\alpha$  satellite ration with and without the titanium layer. Albeit that deconvolution from the merging O-like feature was difficult without titanium (see Fig. 1), we did not find any significant

difference in the two cases. Other possibilities, such as the neglect of electron correlations, an improved treatment of shake-off electron probabilities, or the possibility of a direct collision between the  $1s$  electron and one of the  $L$ -shell electrons of the same atom, have been previously discussed [23].

## CONCLUSIONS

The  $KL$  satellites of aluminum excited by the suprathermal electrons generated during the interaction of an intense subpicosecond laser pulse with a metallic aluminum target have been observed. Their relative intensity to the  $K\alpha$  line was found to be 30% larger than the one measured by conventional x-ray tube or electron-beam excitation. Electron shake-off processes in which the removal of a  $1s$  electron occurs simultaneously with the removal of a  $2s$  or  $2p$  subshell electron were found earlier to account for about 80% of the measured  $KL$  satellite intensities. In order to evaluate the effect of the heating of the target by the intense suprathermal electron flux, a two-step population mechanism of the upper  $(1s2s)^{-1}$  and  $(1s2p)^{-1}$  configurations of the  $KL$  transitions was investigated. Collisional-radiative calculations and synthetic spectra construction have shown that an upper limit of 20 eV should be set for the electron temperature. This value was found to be consistent with the temperature inferred from the experimentally determined electron energy deposition. Experiments are in progress to obtain an independent determination of the electron temperature from the amplitude and the phase shift [33,34] of a  $\approx 100$  fs probe pulse reflected from the rear side of the target [35]. Finally, we would like to stress the point that changing electron excitation conditions of the  $K$  satellites from dc to 100 fs (more than 13 orders of magnitude) changes the  $KL$  satellite intensity by no more than a few percent.

## ACKNOWLEDGMENTS

We wish to acknowledge the very generous help of M. Klapisch in the use of the HULLAC computer code. J.C.G. is deeply indebted to Teijo Åberg for pointing out very interesting references on the early  $KL$  satellite measurements. This work was supported by the Centre National de la Recherche Scientifique and by a EEC grant of the "Human Capital and Mobility Program." One of us (R.M.) acknowledges support from a NSF EPSCOR grant.

- [1] M. M. Murnane, H. C. Kaypten, and R. W. Falcone, *IEEE J. Quantum Electron.* **25**, 2417 (1989).
- [2] M. M. Murnane, H. C. Kaypten, M. D. Rosen, and R. W. Falcone, *Science* **251**, 531 (1991).
- [3] J. C. Kieffer, M. Chaker, J. P. Matte, H. Pépin, Y. Coté, Y. Beaudoin, T. W. Johnston, C. Y. Chien, S. Coe, G. Mourou, and O. Peyrusse, *Phys. Fluids B* **5**, 2330 (1993).
- [4] M. Rosen, *SPIE J.* **1229**, 160 (1990).

- [5] H. M. Milchberg, I. Lyubomirsky, and C. G. Durfee III, *Phys. Rev. Lett.* **67**, 2564 (1991).
- [6] W. Rozmus and V. T. Tikhonchuk, *Phys. Rev. A* **46**, 7810 (1992).
- [7] H. Chen, B. Soon, B. Yaakobi, S. Uchida, and D. D. Meyerhofer, *Phys. Rev. Lett.* **70**, 3431 (1993).
- [8] O. Peyrusse, J. C. Kieffer, C. Y. Coté, and M. Chaker, *J. Phys. B* **26**, L511 (1993).

- [9] R. C. Mancini, P. Audebert, J. P. Geindre, A. Rouse, F. Fallières, J. C. Gauthier, A. Mysyrowicz, J. P. Chambaret, and A. Antonetti, *J. Phys. B* **27**, 1671 (1994).
- [10] P. Audebert, J. P. Geindre, A. Rouse, F. Fallières, J. C. Gauthier, A. Mysyrowicz, G. Grillon, and A. Antonetti, *J. Phys. B* **27**, 3303 (1994).
- [11] F. Brunel, *Phys. Rev. Lett.* **59**, 52 (1987).
- [12] P. Gibbon and A. R. Bell, *Phys. Rev. Lett.* **68**, 1535 (1992).
- [13] A. Rouse, P. Audebert, J. P. Geindre, F. Fallières, J. C. Gauthier, A. Mysyrowicz, G. Grillon, and A. Antonetti, *Phys. Rev. E* **50**, 2200 (1994).
- [14] D. D. Meyerhofer, H. Chen, J. A. Delettrez, B. Soom, S. Uchida, and B. Yaakobi, *Phys. Fluids B* **5**, 2584 (1993).
- [15] J. D. Kmetec, *IEEE J. Quantum Electron.* **28**, 2382 (1992).
- [16] P. Audebert, J. P. Geindre, J. C. Gauthier, A. Mysyrowicz, J. P. Chambaret, and A. Antonetti, *Europhys. Lett.* **19**, 189 (1992).
- [17] A. Rouse, A. Antonetti, P. Audebert, A. Dos Santos, F. Fallières, J. P. Geindre, G. Grillon, A. Mysyrowicz, and J. C. Gauthier, *J. Phys. B* **27**, L697 (1994).
- [18] E. Mikkola, O. Keski-Rahkonen, J. Lahtinen, and K. Reinikainen, *Phys. Scr.* **28**, 188 (1983).
- [19] A. Rouse, F. Fallières, J. P. Geindre, P. Audebert, J. C. Gauthier, A. Mysyrowicz, G. Grillon, J. P. Chambaret, and A. Antonetti, in *OSA Proceedings on Short Wavelength V*, edited by P. B. Corkum and M. D. Perry (Optical Society of America, Washington, DC, 1993), Vol. 17, p. 185.
- [20] A. Rouse, thèse de doctorat, Université Paris-Sud, 1994 (unpublished).
- [21] Ping Wang, J. MacFarlane, and G. A. Moses, *Phys. Rev. E* **48**, 3934 (1993).
- [22] A. K. Agarwal, *X-ray Spectroscopy* (Springer-Verlag, Berlin, 1979), p. 207.
- [23] T. A. Carlson and M. O. Krause, *Phys. Rev.* **140**, A1057 (1965).
- [24] M. O. Krause and J. G. Ferreira, *J. Phys. B* **8**, 2007 (1975).
- [25] Teijo Åberg, *Phys. Rev.* **156**, 35 (1967).
- [26] O. Keski-Rahkonen, K. Reinikainen, and E. Mikkola, *Phys. Scr.* **28**, 179 (1983).
- [27] M. O. Krause, *J. Phys. Chem. Ref. Data* **8**, 307 (1979).
- [28] M. Klapisch, J. L. Schwob, B. S. Fraenkel, and J. Oreg, *J. Opt. Soc. Am.* **67**, 148 (1977).
- [29] A. Bar-Shalom, M. Klapisch, and J. Oreg, *Phys. Rev. A* **38**, 1773 (1988).
- [30] A. Bar-Shalom and M. Klapisch, *Comput. Phys. Commun.* **50**, 375 (1988).
- [31] F. Hopkins, D. O. Elliot, C. P. Bhalla, and P. Richard, *Phys. Rev. A* **8**, 2952 (1973).
- [32] I. I. Sobelman, *Introduction to the Theory of Atomic Spectra* (Pergamon, Oxford, 1972), p. 256.
- [33] J. P. Geindre, P. Audebert, A. Rouse, F. Fallières, J. C. Gauthier, A. Mysyrowicz, A. Dos Santos, G. Hamoniaux, and A. Antonetti, *Opt. Lett.* **19**, 1997 (1994).
- [34] P. Audebert, P. Daguzan, A. Dos Santos, J. C. Gauthier, J. P. Geindre, S. Guizard, G. Hamoniaux, K. Krastev, P. Martin, G. Petite, and A. Antonetti, *Phys. Rev. Lett.* **73**, 1990 (1994).
- [35] B.-T. V. Vu, A. Szoke, and O. L. Landen, *Phys. Rev. Lett.* **72**, 3823 (1994).